Available online at www.sciencedirect.com

SCIENCE DIRECT®

Biochimica et Biophysica Acta 1604 (2003) 105–114

BIOCHIMICA ET BIOPHYSICA ACTA

BBA

www.bba-direct.com

Mechanics and structure of titin oligomers explored with atomic force microscopy

Miklós S.Z. Kellermayer[a,*], Carlos Bustamante[b], Henk L. Granzier[c]

[a] *Department of Biophysics, Faculty of Medicine, University of Pécs Medical School, Szigeti ut 12., Pécs, H-7626 Hungary*
[b] *Department of Physics, Howard Hughes Medical Institute, University of California, Berkeley, CA 94720, USA*
[c] *Department of VCAPP, Washington State University, Pullman, WA 99164, USA*

Received 16 July 2002; received in revised form 5 March 2003; accepted 25 March 2003

Abstract

Titin is a giant polypeptide that spans half of the striated muscle sarcomere and generates passive force upon stretch. To explore the elastic response and structure of single molecules and oligomers of titin, we carried out molecular force spectroscopy and atomic force microscopy (AFM) on purified full-length skeletal-muscle titin. From the force data, apparent persistence lengths as long as ~1.5 nm were obtained for the single, unfolded titin molecule. Furthermore, data suggest that titin molecules may globally associate into oligomers which mechanically behave as independent wormlike chains (WLCs). Consistent with this, AFM of surface-adsorbed titin molecules revealed the presence of oligomers. Although oligomers may form globally via head-to-head association of titin, the constituent molecules otherwise appear independent from each other along their contour. Based on the global association but local independence of titin molecules, we discuss a mechanical model of the sarcomere in which titin molecules with different contour lengths, corresponding to different isoforms, are held in a lattice. The net force response of aligned titin molecules is determined by the persistence length of the tandemly arranged, different WLC components of the individual molecules, the ratio of their overall contour lengths, and by domain unfolding events. Biased domain unfolding in mechanically selected constituent molecules may serve as a compensatory mechanism for contour- and persistence-length differences. Variation in the ratio and contour length of the component chains may provide mechanisms for the fine-tuning of the sarcomeric passive force response.

Keywords: Titin; Wormlike chain; Unfolding; Elasticity; AFM; Molecular force spectroscopy

1. Introduction

When a nonactivated striated muscle cell is stretched, passive force develops which restores muscle length following release. During active muscle contraction, passive force limits sarcomere-length inhomogeneity along the muscle cell and limits A-band asymmetry within the sarcomere [1,2]. One of the main determinants of passive muscle force is the filamentous intrasarcomeric protein titin [3], a 3.0- to 3.7-million-dalton protein (for recent reviews, see Refs. [4–6]) that spans the half sarcomere [7,8]. Titin is anchored to the Z-line and to the M-line and is attached to the thick filaments of the A-band. The I-band segment of the molecule is constructed of serially linked immunoglobulin (Ig)-like domains interspersed with unique sequences including a proline (P)-, glutamate (E)-, valine (V)-, and lysine (K)-rich PEVK domain [8]. Upon stretch of the sarcomere, passive force is generated by the extension of the I-band segment of titin [9–11]. Recent findings suggest that the I-band may contain isoforms of different lengths [12], which are, by definition, confined to the same structural framework of the sarcomere. However, the intermolecular relationship between the constituent titins and the effect of length-isoform variation on sarcomeric passive force generation are not precisely known.

In the present work, we carried out molecular force spectroscopy and atomic force microscopy (AFM) on full-length, purified skeletal muscle titin. We observe that titin molecules may be globally associated into oligomers which, in the context of a stretching experiment, behave as aligned, independent wormlike chains (WLCs). The mechanical data suggest that the apparent overall persistence length of full-length unfolded titin may be up to 1.5 nm, and that oligomers containing six-component molecules might represent a rel-

* Corresponding author. Tel.: +36-72-536-271; fax: +36-72-536-261.
E-mail address: Miklos.Kellermayer.Jr@aok.pte.hu (M.S.Z. Kellermayer).

0005-2728/03/$ - see front matter © 2003 Elsevier Science B.V. All rights reserved.
doi:10.1016/S0005-2728(03)00029-X

atively stable supramolecular arrangement. AFM microscopic data indicate that although oligomers may form via head-to-head association of titin, along their contour, the molecules are independent from each other. Simulations based on a model of independent WLCs arranged in parallel allowed us to calculate the net mechanical behavior of sarcomeres containing length isoforms of titin.

2. Materials and methods

2.1. Protein preparation

Titin was prepared from rabbit m. longissimus dorsi by using previously published protocols [13,14]. The protein samples were stored, before use, on ice in "CB buffer" (30 mM K-phosphate, pH 7.0, 0.6 M KCl, 0.1 mM EGTA, 0.3 mM DTT, 0.1% NaN_3, 40 μg/ml Leupeptin, and 20 μM E-64 and 0.05% Tween-20). Typical T1 (full-length molecule) to T2 (major proteolytic fragment) ratios ranged beween 1 and 0.3. An SDS-PAGE pattern with a T1/T2 ratio of 0.3 is shown in Fig. 1a, inset.

2.2. Mechanical manipulation of titin

Titin molecules were mechanically stretched by using a Molecular Force Probe (MFP, Asylum Research, Santa Barbara, CA). The MFP was mounted on a custom-built, low-profile inverted light microscope. Titin, diluted in assay buffer ("AB," 25 mM imidazole–HCl, pH 7.4, 0.2 M KCl, 4 mM $MgCl_2$, 1 mM EGTA, 0.01% NaN_3, 1 mM DTT, 20 μg/ml Leupeptin, 10 μM E-64), was allowed to bind to a precleaned glass microscope slide for 10 min. Unbound molecules were washed away with AB buffer. The molecules were stretched in AB solution by first pressing a cantilever (#MSCT AUHW, ThermoMicroscopes, or BioLever, Olympus) against the titin-coated surface, then pulling it away with a predetermined rate (typical stretch rate, 1 μm/s). Force vs. displacement curves were collected in repeated stretch and release cycles. The displacement of the cantilever base was measured by using an integrated linear voltage differential transformer (LVDT). Force (F) was obtained from cantilever bending (Δd) as

$$F = K\Delta d, \tag{1}$$

where K is cantilever stiffness. Stiffness was obtained for each unloaded cantilever by measuring its thermally driven mean-square vertical displacement and applying the equipartition theorem:

$$K\langle \Delta d^2 \rangle = k_B T, \tag{2}$$

where k_B is Boltzmann's constant and T is absolute temperature. Force vs. displacement curves were corrected for several factors to obtain force vs. molecular end-to-end length: (1) The zero-length, zero-force data point was obtained from the force response that corresponded to the cantilever tip reaching (or departing from) the substrate surface. (2) Forces were corrected for baseline slope obtained from the force response of the displaced but unloaded

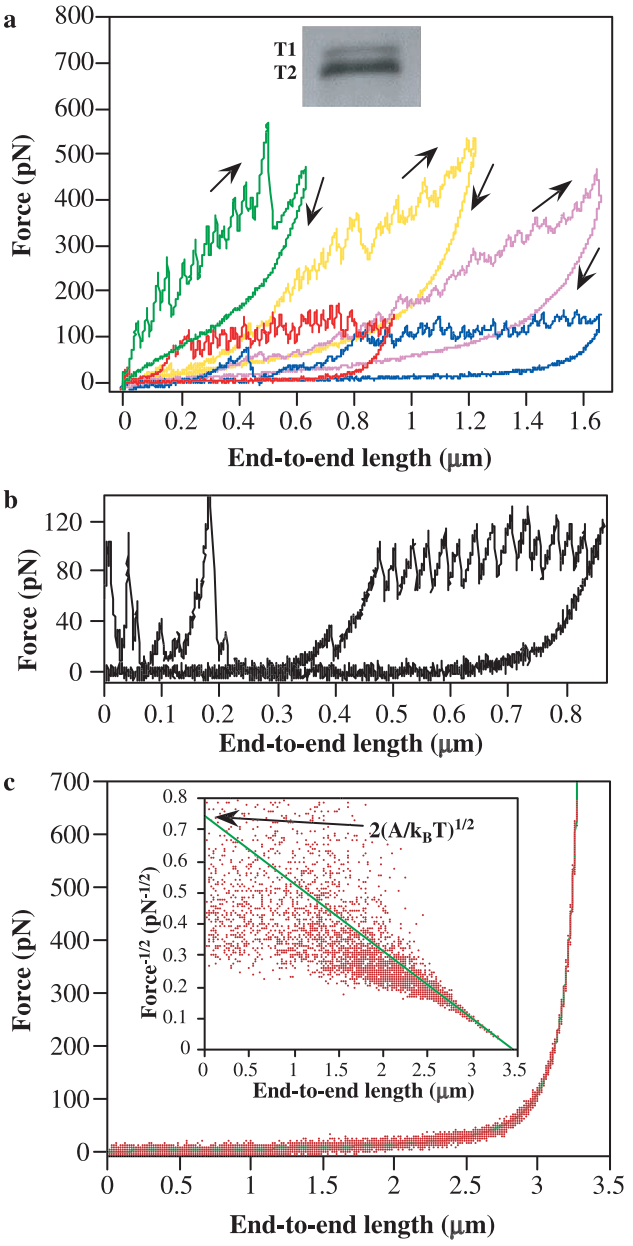

Fig. 1. (a) Representative force vs. end-to-end length curves obtained during titin stretching with the MFP. Arrows indicate direction of data acquisition (stretch or release). Mean stretch rate, 1 μm/s. Inset: Silver-stained SDS-PAGE pattern [44] of a titin preparation with a T1/T2 ratio of 0.3. (b) Force vs. end-to-end length of a titin molecule in which equally spaced repetitive force peaks appeared. (c) Analysis of the data by using a nonlinear least squares (Marquardt–Levenberg) fit of the WLC equation onto the force curve or a linear fit onto the force$^{-1/2}$ data set (inset). The x- and y-axis intercepts of the extrapolated linear fit allow a direct determination of characteristic features, the contour (L) and persistence lengths (A), of the WLC.

cantilever. (3) The end-to-end length (z) of the tethered molecule was calculated by correcting the cantilever base displacement (s) with cantilever bending as

$$z = s - \frac{F}{K}. \tag{3}$$

2.3. Analysis of force data

Force data were compared with the WLC equation [15,16]

$$\frac{FA}{k_B T} = \frac{z}{L} + \frac{1}{4(1 - z/L)^2} - \frac{1}{4} \tag{4}$$

where A and L are the apparent persistence and contour lengths of the tethered molecule, respectively. The experimental curves were fitted with the WLC equation by using a nonlinear least squares fit (Marquardt–Levenberg, see Fig. 1c). Alternatively, a linear function was fitted on the high fractional extension ($z/L > \sim 0.8$) region of force$^{-1/2}$ vs. end-to-end length data (see Fig. 1c, inset) [17,18]. The x- (i.e., end-to-end length) axis intercept of the linear function provides the contour length. The y- ($F^{-1/2}$) axis intercept (F_{int}), on the other hand, allows the apparent persistence length of the titin tether to be calculated as

$$A = \frac{k_B T}{4F_{int}}. \tag{5}$$

The above analysis was utilized to (1) identify apparent WLC behavior during the stretch–release cycle, (2) find the apparent persistence length of partially unfolded titin during stretch, and (3) calculate the apparent persistence length of the unfolded titin molecule from the release data. The persistence length of the single, mechanically unfolded titin molecule (A_0) was obtained from the statistical distribution of the apparent persistence length (A) derived from the release portion of many stretch–release experiments. A_0 was identified as the length corresponding to the histogram peak at the longest apparent persistence length. The force required to produce a given fractional extension of tethers made up of n parallel molecules is n times that required to induce the same fractional extension on a single molecule. Then, based on Eq. (5), the number of molecules in any titin tether can be calculated from the value of its persistence length A derived from the experimental force–extension curve as

$$n = \frac{A_0}{A}. \tag{6}$$

2.4. Atomic force microscopy

A 10-μl sample of titin, diluted in AB buffer, was applied to a freshly cleaved mica surface and incubated for 10 min. Unbound molecules were washed away with AB buffer, then the surface was rinsed with distilled water and dried with nitrogen gas. Surface-adsorbed molecules were imaged with a Nanoscope III (Digital Instruments) using silicon tips (Nanosensors) in tapping mode. Typical scanning rates were 1.5 Hz. The acquired images were imported into and analyzed with Image 1.61 software (Wayne Rasband, NIH). For spatial calibration, the internal calibration of the AFM was used. The persistence length (A) of the surface-adsorbed titin molecules was calculated from the two-dimensional mean square end-to-end distance ($\langle R^2 \rangle_{2D}$) and the contour length (L) [19]. The axial height distribution along the titin molecule was obtained by manually tracking its contour and then assembling a profile plot using the height calibration of the Nanoscope instrument. Autocorrelation of the axial height data was performed by using IgorPro software (Wavemetrics, Lake Oswego, OR).

2.5. Modeling, simulation, and theory

To model force-driven domain unfolding/refolding in a tether containing more than one titin molecule, Monte-Carlo simulations were carried out based on previously used simulation algorithms [17,20]. The mechanical behavior of titin was simulated by superimposing the domain unfolding/refolding kinetics on WLC behavior. In simulating titin's mechanical behavior, we considered the molecule as a serially linked chain containing segments with different persistence lengths. As a titin molecule is mechanically stretched and becomes gradually unfolded, its contour length exceeds that of the native molecule (~ 1 μm [21]) and approaches the length of titin's primary structure (~ 10 μm [8]). In addition, the apparent persistence length (A) decreases as the rigid native molecule ($A_{folded} \sim 15$ nm [22]) is converted into the flexible unfolded ($A_{unfolded} \sim 1.5$ nm [20]).

For a tether containing two titins, the mechanical response was simulated by independently calculating the instantaneous forces in each molecule. Net force was obtained by summing the component forces (F_i) calculated for the molecules. At each step, for the given F_i, the number of domains unfolded/refolded was calculated for each titin according to

$$dN_i = N_i \omega_0 dt e^{-(E_a - F_i \Delta x)/k_B T}, \tag{7}$$

where, for the ith molecule, dN_i is the change in the number of folded domains during the dt polling interval and N_i is the number of available folded domains. ω_0, attempt frequency, was 10^8 [23], and $k_B T$ was 4.14 pN nm. Note that for short dt, dN_i corresponds to the probability that any one domain becomes unfolded during dt at the given instantaneous force. Typical unfolding and refolding activation energies (E_a) used were 128 and 83 pN nm, respectively [24,25]. Typical unfolding and refolding potential widths (Δx) were 0.3 and 8 nm, respectively [17,25]. Following each calcu-

lation step, the domain unfolding process was permitted or prohibited depending on a comparison of dN_i with a number generated randomly between 0 and 1. Unfolding events decreased the number of remaining folded domains, reduced the length of the folded segment by 4 nm, and increased the length of the unfolded segment by 30 nm. Refolding events increased the number of folded domains, increased the length of the folded segment by 4 nm, and decreased the length of the unfolded segment by 30 nm. The apparent persistence length of the simulated titin molecules was calculated from the force$^{-1/2}$ vs. end-to-end length curves according to Eq. (5).

To calculate—from component chain parameters—the apparent persistence length (A_{app}) of a tether containing two molecules with *unequal* contour lengths (L_{long} and L_{short}), we derived a simplified equation based on the following assumptions: (a) the persistence lengths of the component chains are identical (A); (b) the end-to-end distances of the component chains are equal (z) because they are confined to the same lattice; (c) neither of the component chains rupture during extension, therefore the contour length of the tether is identical to that of the shorter chain ($L_{tether}=L_{short}$); and (d) the force of the tether is the sum of the forces of the component chains ($F_{tether}=F_{short}+F_{long}$). Accordingly, A_{app} can be determined as

$$\frac{1}{A_{app}}=\frac{1}{A}+\frac{1}{A}\frac{\left[\frac{z}{L_{long}}+\frac{1}{4\left(1-\frac{z}{L_{long}}\right)^2}-\frac{1}{4}\right]}{\left[\frac{z}{L_{short}}+\frac{1}{4\left(1-\frac{z}{L_{short}}\right)^2}-\frac{1}{4}\right]}. \quad (8)$$

The two limits of possible arrangements in such a titin doublet are that (a) if the component chains have equal contour lengths ($L_{long}=L_{short}$), or (b) if the contour length of one chain far exceeds that of the other ($L_{long}\gg L_{short}$). If $L_{long}=L_{short}$, then

$$\frac{1}{A_{app}}=\frac{1}{A}+\frac{1}{A}=\frac{2}{A}, \quad (9)$$

therefore $A_{app}=A/2$. If, on the other hand, $L_{long}\gg L_{short}$, then $L_{long}\gg z$, and

$$\frac{1}{A_{app}}=\frac{1}{A}, \quad (10)$$

therefore $A_{app}=A$. Calculations and simulations were carried out by using Object Pascal (Metrowerks CodeWarrior v.10) on a Power Macintosh G4 Computer.

3. Results

3.1. Force vs. extension curves of titin molecules

Titin molecules, prepared from rabbit back muscle, were stretched and then released. An ensemble of force vs. end-to-end length curves of different titin tethers is shown in Fig. 1a. The force curves reveal that: (1) there is a variation in the maximal end-to-end length, which is most likely due to capturing different portions of the molecule; (2) there are significant differences in the force levels for a given fractional extension, suggesting that a varying number of molecules are tethered *in or nearly parallel*; (3) the stretch data contain repetitive (sometimes equally spaced, Fig. 1b) force peaks that correspond to individual domain unfolding events [26]; and (4) each data set contains force hysteresis, indicating that the system is being extended away from equilibrium.

3.2. Titin as an WLC entropic polymer

To measure the elastic properties of titin during mechanical manipulation, the release data were compared with the predictions of the WLC theory [15,16] and models of serially linked WLCs [27,28]. Two methods were employed: (a) nonlinear least squares fit (Fig. 1c) to the force vs. end-to-end length curve or (b) a linear fit to the force$^{-1/2}$ vs. end-to-end length data (Fig. 1c, inset). Both approaches gave identical results. The excellent fit of the WLC theory indicates that in the release part of the mechanical cycle, the titin tether can be well described as an entropic, WLC (equilibrium) model [20]; therefore, this regime describes the purely elastic behavior of a partially or completely [29] unfolded titin tether.

3.3. Mechanical properties of titin oligomers

To describe the elastic properties of the unfolded titin molecule, we calculated the apparent persistence length distribution obtained from many release data sets (Fig. 2a). The apparent persistence length histogram is a multimodal distribution with peaks corresponding to the number of molecules within the tether. The expected discrete distribution is distorted, probably due to the presence of partially unfolded molecules, tethers containing molecules of unequal length, and variation of the persistence length of a molecule along its contour (see Discussion). The peak at the longest apparent persistence length is likely to correspond to the single unfolded titin molecule. Based on this approach, the persistence length of the single unfolded titin molecule may be up to ~1.5 nm. The number of titin molecules in the tether was calculated based on the derived persistence length for the single titin molecule (Fig. 2b). A multimodal distribution is observed with peaks corresponding to tethers containing different numbers of molecules. The frequencies of the number of component molecules are not identical, suggesting that oligomers containing certain

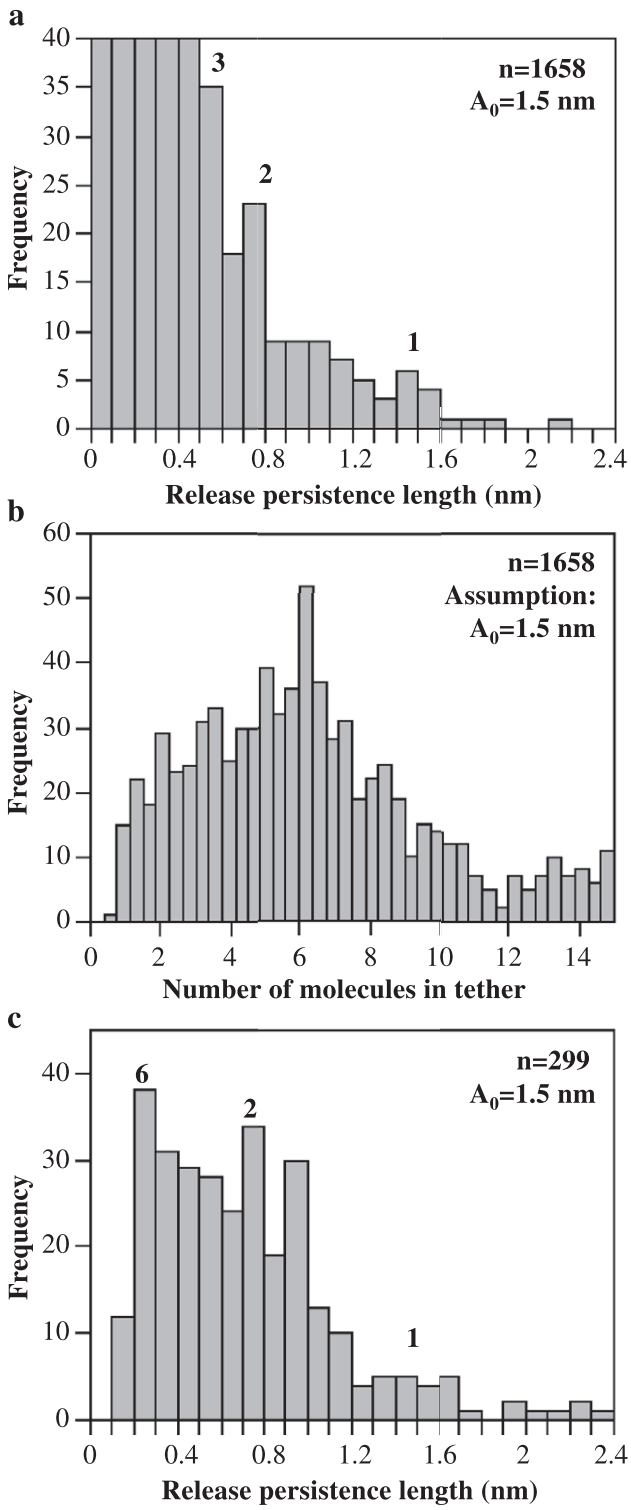

Fig. 2. (a) Distribution of apparent persistence lengths for 1658 release data sets. Numbers above the histogram peaks suggest the corresponding number of molecules within the tether. The persistence length of the single unfolded titin molecule is identified as ~1.5 nm. (b) Distribution of the number of titin molecules within the tether in our experimental data set. The number of molecules was calculated based on the assumption that the persistence length of the single unfolded titin molecule is 1.5 nm. (c) Distribution of apparent persistence lengths in a 100-fold diluted sample.

numbers of molecules might preferentially form. Considering that multimolecular tethers dominated the experimental data set, we mechanically manipulated samples diluted 100-fold to explore whether multiple molecules represented oligomers or simply were due to a nonspecific collection of molecules in a concentrated sample. Fig. 2c shows the results. The distribution of apparent persistence lengths in the range of a few molecules (up to six) is more similar than in Fig. 2a, suggesting that the formation of multimolecular tethers is not entirely due to a random process but that oligomerization of titin has occurred.

A preferred association of titin molecules was also suggested during the repetitive stretch of the same tether to progressively increasing lengths (Fig. 3). In such a tether, a progressive decrease in the number of component molecules was observed, presumably due to the breakage or dissociation of titin from the surface or the cantilever tip. The number of the component titin molecules did not decrease gradually, however, but in discrete steps of more than one molecule. Thus, it appears that as a titin tether is stretched to progressively increasing lengths, component molecules dissociate not one-by-one, but oligomer-by-oligomer.

3.4. AFM of surface-adsorbed titin

The local and global structure surface-adsorbed titin was studied by using tapping-mode AFM on dehydrated samples. Various single, surface-equilibrated titin molecules are shown in Fig. 4a. The molecules display a convoluted structure, which is determined by the bending rigidity of the molecule. Frequently, a globular ‘‘head’’ may be observed at

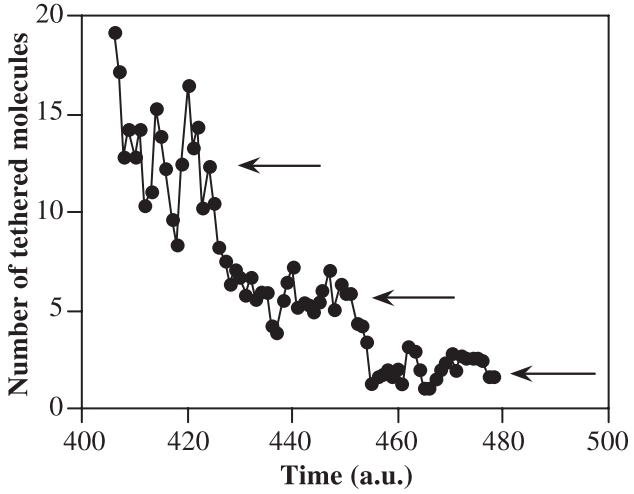

Fig. 3. Number of molecules within the titin tether as a function of time during a titin stretching experiment. Time corresponds to consecutive stretch release cycles to progressively increasing lengths. The apparent persistence length was calculated for each release curve in the respective stretch–release cycle. Arrows point to numbers of titin molecules which apparently form stable tethers. The number of molecules was obtained by using Eq. (6), using 1.5 nm as the persistence length for the single titin molecule.

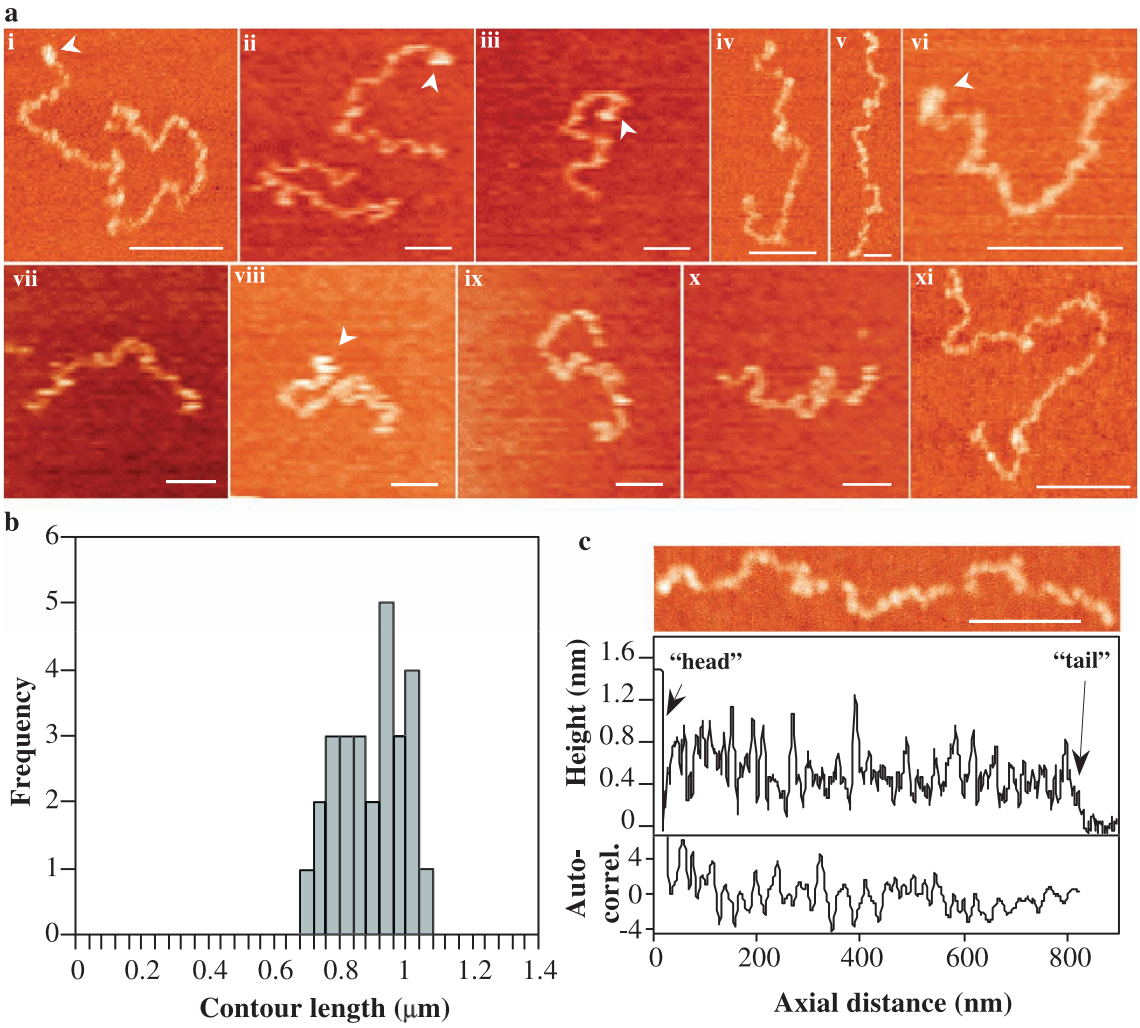

Fig. 4. (a) AFM images of single titin molecules. Globular M-line head is indicated with arrowheads. Scale bar, 0.1 μm. (b) Contour length distribution of titin molecules. (c) Top: Magnified image of a representative titin molecule displaying fluctuations in molecular height. Scale bar, 0.1 μm. Middle: Axial distribution of height for a titin molecule. Bottom: Autocorrelation function of the fluctuation of molecular height around the mean.

one end of the chain (arrowheads), which is likely to correspond to the M-line region of the molecule [21,30]. The contour length distribution of the single titin molecules is shown in Fig. 4b. The mean contour length is 0.87 μm (±0.08 S.D.), suggesting that the chains are full-length titin molecules in the native configuration [31]. The calculated persistence length [19] is 18.7 nm, which corresponds well but slightly exceeds previously measured values (15 nm [22], 13.5 nm [31]). The slight overestimation of the persistence length might be attributed to difficulties in measuring the contour length precisely due to unresolved local structure (see below). The width of the molecules on the images is 7.7 nm (±1.7 S.D.), which far exceeds previous measurements on electron microscopic images (4 nm [32–34]) or the width of a folded globular domain (2 nm [35]). The overestimation of chain width can be attributed to convolution with the finite dimensions of the AFM tip which has a 5- to 10-nm radius of curvature (Nanosensors factory specifications). The mean height along a titin chain is 0.5 nm (±0.2 S.D.), which is smaller than previous measurements of chain diameter (see above) and could be caused by the dehydration process during sample preparation. A magnified AFM image of a titin molecule is shown in Fig. 4c, top, enabling discernment of ultrastructural features. In the height distribution (Fig. 4c, middle) along the contour, peaks and valleys are observed. The autocorrelation function of the relative axial height fluctuation along the molecular axis (Fig. 4c, bottom) reveals a 18.6-nm (±7.9 S.D.) periodicity.

In addition to single molecules, our samples also contained oligomers of titin. A low-magnification field of view acquired with AFM is shown in Fig. 5a. AFM images of various titin oligomers are shown in Fig. 5b. The oligomers range from bi-molecular (Fig. 5b, i–ii) to high-order (Fig. 5b, iii–vii) complexes. In every case, a globular head is observed through which the component titin molecules connect to each other. Notably, the globular head is the only point of attachment between the component titin molecules. The rest of the contour of the individual component titin molecules is

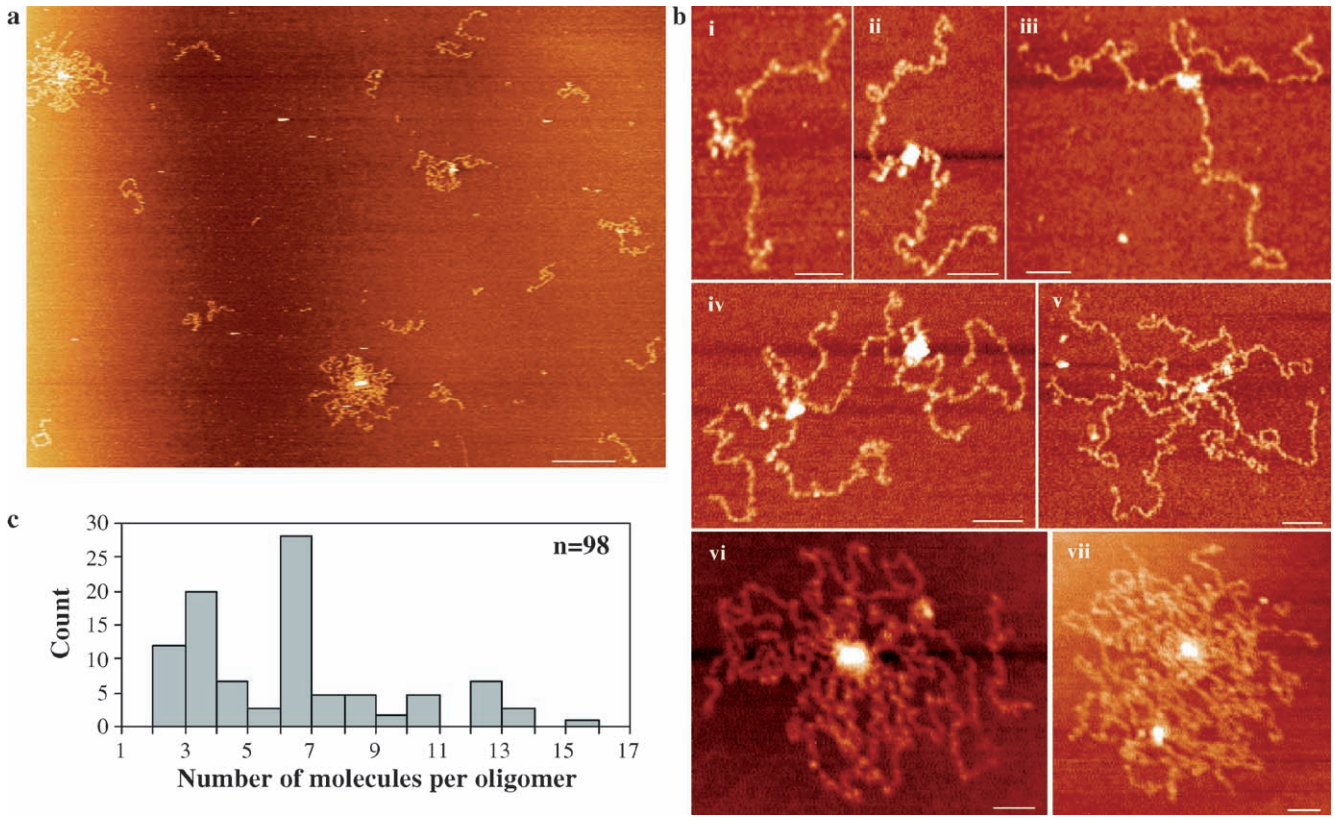

Fig. 5. AFM of titin oligomers. (a) Small magnification overview of a titin-coated mica surface. Scale bar, 0.5 μm. (b) Titin oligomers ranging from bimolecular to high-order complexes. In images iv and vii, two oligomers are lying close to each other. Scale bar, 0.1 μm. (c) Distribution of the number of titin molecules in oligomers in AFM images.

apparently independent, and does not form connections between neighboring molecules within the oligomer. The surface-equilibrated titin oligomers display a radially symmetric global appearance, where the point of symmetry is the globular, presumably M-line-region head. Accordingly, in high-order oligomers (Fig. 5b, iii–vii), the component molecules tend to be evenly distributed around the point of symmetry, further suggesting that they are independent from each other. The distribution of the number of branches, corresponding to constituent titin molecules, counted on the AFM images of oligomers is seen in Fig. 5c. The distribution qualitatively resembles that in Fig. 2b, suggesting that some oligomeric arrangements may be more prevalent.

4. Discussion

We have measured the mechanical properties and structure of skeletal muscle titin molecules and oligomers by using AFM. The AFM method, due to the relatively high typical stiffness of the cantilevers used, allows the mechanical manipulation of multimolecular tethers, which can be stretched with forces up to several nanonewtons. By contrast, with laser tweezers, we could exert forces only up to a few hundred piconewtons [17,18]. The variation in the force level for a given fractional extension (Fig. 1a), seen in the raw force data, can be explained by the variation in the number of titin molecules tethered. Further analysis revealed that the stretched tether may indeed contain many titin molecules (Figs. 2 and 5). The force vs. extension curves contain force peaks which correspond to individual domain unfolding events [26]. The force peaks are typically more or less equally spaced in single-molecule tethers (Fig. 1b), but sometimes even in multi-molecular ones (Fig. 1a, green curve). The presence of unfolding force peaks in multi-molecular titin tethers can be attributed to domain unfolding events in individual component molecules, which behave as independent chains within the tether. The inextensible WLC model was used to fit either the force or the force$^{-1/2}$ data acquired during release for the various multi-molecular tethers. The goodness of the fit further suggests that multi-molecular titin tethers correspond to *parallel or nearly parallel* arrangements of otherwise independent entropic chains.

The persistence length of the single unfolded titin molecule was obtained from the statistical distribution of apparent persistence lengths obtained in many stretch–release experiments (Fig. 2a). In the data set, the peak at the longest apparent persistence length is seen at ~1.5 nm, and persistence lengths up to 2.4 nm may be seen on occasion (Fig. 2c). We tentatively assign 1.5 nm to the overall, apparent persistence length of the unfolded titin molecule. Previous single-molecule studies estimated the persistence length of the

unfolded titin molecule (2 nm [17], 1.6 nm [20], 0.76 nm [36]), recombinant I91-98 tandem Ig segment (0.4 nm [26], 0.6 nm [37]), I65-70 tandem Ig segment (0.6 nm [37]), tandem FNIII domains (0.4–0.8 nm [25]), engineered, mutant Ig polyproteins (0.35 nm [38]), cardiac PEVK segment (0.4–2.5 nm [39], 1.4 nm [40]), and the cardiac N2B unique sequence (0.65 nm [40]). Considering that of the various segments in titin only the persistence length of the PEVK segment is comparable to the persistence length of the full-length titin observed here, it is conceivable that many of the captured titin molecules were dominated by the PEVK segment. Segments that remained in the native configuration (persistence length 13–18 nm [22,31] and present results) may have also contributed to the relatively long persistence length. The additional, broadened histogram peaks at shorter persistence lengths are interpreted to correspond to an integer multiple of titin molecules in the tether. There is a variation of the apparent persistence length around the mean value for the given number of molecules within the tether. The most likely contributors to such variation are: (a) variation in the degree of unfolding (remaining folded segments increase the apparent persistence length); (b) differences in the contour lengths of the titin molecules in the parallel arrangement (a short component chain contributes more significantly towards net force); (c) different sections of the molecule, having different local persistence lengths, might have been captured; (d) molecular arrangement in the captured oligomer (a single titin molecule held by the tip at its non-M-line end could be tethered to the surface by the rest of the molecules of the oligomer); and (e) the geometry of molecule stretching (error in determining the contour length caused by a deviation from 90° of the incident angle, i.e., the angle between the surface and the molecular axis). In the extreme case of ~45° incident angle [calculated as the inverse tangent of the ratio of minimal cantilever height in the data set (~0.2 μm) and the mean end-to-end distance of the surface-adsorbed titin molecule (~0.2 μm)], this error is only ~4% [38].

The persistence length of the single titin molecule allows us to calculate the number of titin molecules in any tether from its apparent persistence length (assuming that all have the same persistence length). The distribution of the number of molecules (Fig. 2b) displays a multimodal histogram with peaks corresponding to particular integer multiples of titin molecules. The histogram deviates from the expected Poisson distribution suggesting that the events of titin attachment to the cantilever tip are not independent and random. This behavior could be caused by a global association of titin molecules into oligomers. Thus, multimolecular tethers may represent oligomers of titin. It is unlikely that the multimolecular tethers arise from a nonspecific aggregation of titin molecules captured by the tip, because a similar apparent persistence length distribution is observed in a sample diluted 100-fold (Fig. 2c). Titin oligomerization is also suggested in case of tethers stretched to progressively increasing lengths (Fig. 3). As the tether is stretched further and further, more and more molecules break off the AFM tip, leaving behind less and less titins within the tether. The titin molecules apparently dissociate from the tether not one-by-one, but group-by-group, possibly oligomer-by-oligomer. The observation suggests that the most likely point of attachment to (and hence detachment from) the tethering surface is the globular head, a possibility raised in earlier molecular combing experiments [21]. Figs. 2b–c and 3 indicate that most frequently the titin oligomers contain six molecules, although different scenarios also prevail (see Fig. 5).

The tapping-mode AFM images of surface-adsorbed titin molecules (Fig. 4) reveal an appearance similar to that seen in electron micrographs [31]. Repetitive peaks in molecular height appear along the molecular axis (Fig. 4c, middle) with a periodicity (18.6±7.9 nm) that exceeds inter-domain spacing [35]. Presently, we speculate that the repetitive structural arrangements involve a preferred arrangement of specific groups of neighboring domains (e.g., super-repeat). More detailed work is required to determine the origin of the repetitive height peaks and to understand the exact supra-domain structure in titin. The titin samples examined contained a fraction of oligomers (Fig. 5) ranging between bimolecular and high-order complexes. Whether the number and arrangement of titin in these dehydrated specimens correspond well to those in the mechanical experiments needs to be established; however, the images clearly demonstrate titin oligomerization. In oligomers, the component molecules radiate from a globular head which most likely corresponds to the M-line end of titin [21]. As the size of the central head apparently increases with the number of component molecules, it appears to form by the association of individual M-line heads. The titin oligomers display a radial symmetry, and the component molecules are evenly distributed around the central globular head. The radial distribution of component molecules and the lack of association between them further along their contour suggest that apart from a head-to-head association, the titin molecules are independent from each other in the oligomer under the experimental conditions used here (0.2 M KCl). Thus, while titin molecules may be associated on the global scale, they are independent elastic chains on the local scale. Based on the mechanical data and the distribution of the number of branches in titin oligomers counted on AFM images (Fig. 5c), we tentatively draw the conclusion that a titin oligomer containing six molecules might represent a relatively stable arrangement.

The observation of the axial structural and mechanical independence of titin molecules within an oligomer permits the theoretical consideration of possible mechanisms and simulation of net sarcomeric elasticity. In case of the single titin molecule, the overall apparent elasticity is determined by its contributing segments (contour and persistence lengths of native and unfolded Ig domains, PEVK and other unique-sequence elements). Thus, the elastic I-band section of titin is a serially linked chain composed of segments with different persistence lengths [27,41]. The net force gener-

ated by the elastic I-band titin section can be calculated from the fractional extension and persistence lengths of the component segments. In case of titin oligomers, and eventually of the sarcomere, the apparent elasticity is determined by the sum of the forces contributed by each of the molecules aligned near parallel. In a lattice that contains several independent WLCs of different contour lengths (L) arranged in parallel and stretched to the same end-to-end length (z), each chain assumes an equilibrium configuration of highest entropy, and will contribute to the net force according to its fractional extension (z/L). To estimate the combined effect of unequal contour lengths and domain unfolding (i.e., progressive change in the variation of persistence length along the chain's contour) on the apparent persistence length of a titin tether, we simulated the mechanical behavior of a doublet of titin molecules in which the initial contour length and the number of folded domains of the component molecules were different (Fig. 6a). As the extension of the tether increased, the number of folded domains progressively decreased, and this resulted in a decrease in the tether's apparent persistence length. Interestingly, the rapid decrease in apparent persistence length was accompanied by progressive unfolding in only one of the component molecules (the component molecule with the shorter apparent contour length). Once the numbers of unfolded domains in the two molecules were similar, further decrease in apparent persistence slowed down significantly. Apparently, a differential (biased) domain unfolding may compensate for contour and persistence length differences between different titin molecules tethered in parallel. Conceivably, such a biased domain unfolding may compensate for titin isoform variation and for local fluctuations in the mechanical behavior in situ in the sarcomere.

There is an increasing amount of evidence that the half sarcomere may contain titin isoforms with significantly different contour lengths [12,42]. In the bovine ventricle, the shorter N2B and the longer N2BA isoforms are expressed mutually in the half sarcomere (see Fig. 6b). It has been shown that these isoforms extend independently [42]. The axial independence of titin molecules within the oligomer observed here and the independent extensibility of titins in the sarcomere probably derive from the same structural properties of titin. Considering the independence of component molecules, the lateral association of titin molecules into junction lines [34] or end-filaments [43] seen earlier in the I-band may be evoked by extramolecular factors (e.g., ionic milieu, titin-associated proteins). We used

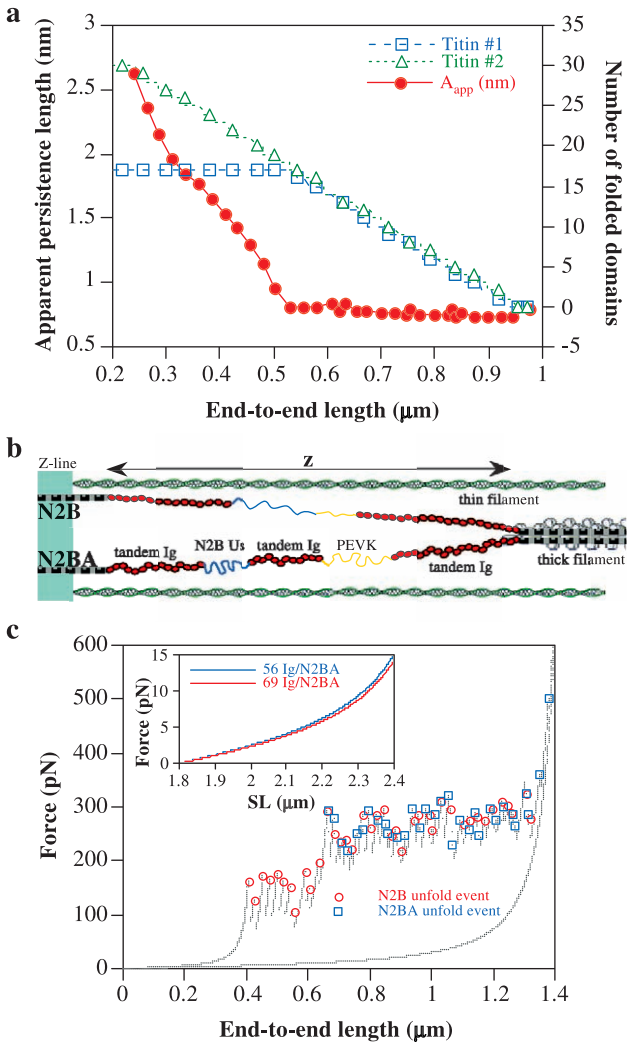

Fig. 6. Simulation of titin's mechanical behavior using WLC elasticity and domain folding/unfolding kinetics. (a) Apparent persistence length of a titin doublet as a function of end-to-end length during simulated mechanical stretch. The titin molecules in the model doublet contained different number of domains and a preunfolded segment with different length at the beginning of stretch. Open squares and triangles correspond to the number of remaining folded domains in the first and second molecule, respectively. Initial parameters of the simulated molecules: Molecule #1, 17 folded domains, 500-nm-long preunfolded segment. Molecule #2, 30 folded domains, 220-nm-long preunfolded segment. Persistence lengths were 15 nm for folded titin and 1.5 nm for unfolded titin. Simulation parameters: polling interval 0.001 s, cantilever stiffness 10 pN/nm, stretch rate 500 nm/s, unfolding activation energy 128 pN nm, refolding activation energy 83 pN nm. Apparently, domain unfolding in one of the titin molecules compensates for differences in the contour and persistence lengths between the two molecules. (b) Schematics of arrangement of N2B and N2BA isoforms of titin in the half sarcomere. (c) Simulation results for a stretched doublet containing the elastic sections of one N2B and one N2BA isoform. The N2B isoform contained 40 Ig domains, a 217-nm-long N2B unique sequence (N2B Us), and a 63-nm-long PEVK segment. The N2BA isoform contained 69 Ig domains, a 217-nm-long N2B Us, and a 228-nm-long PEVK segment. The persistence lengths for the folded tandem Ig, the unfolded Ig, the N2B Us, and the PEVK segments were 15 nm [22], 0.65 nm [37], 0.65 nm, [40] and 14 nm [40], respectively. Domain unfolding events are indicated with red circles and blue squares for the N2B and N2BA isoforms, respectively. Monte-Carlo simulation parameters: polling interval 0.001 s, cantilever stiffness 10 pN/nm, stretch rate 500 nm/s, unfolding activation energy 128 pN nm, refolding activation energy 83 pN nm (see Section 2 for details). Inset: Effect of variation in length of the extra tandem Ig insert in N2BA isoform on the apparent elasticity of a bi-molecular tether containing one N2B and one N2BA isoform. The effect of the shortest (12 extra Ig domains, total 56 domains, blue line) and longest (25 extra domains, total 69 domains, red line) N2BA isoforms are compared [45].

the above model and simulation algorithms to predict the mechanical behavior of a two-molecule titin tether containing one N2B and one N2BA isoform (Fig. 6c). In the beginning of stretch, an apparent elasticity determined by the apparent persistence lengths of the component chains is observed. Subsequently, domain unfolding events begin to occur first in the shorter, N2B isoform only, then unfolding proceeds in both isoforms simultaneously (red circles and blue squares). The intitial domain unfolding in the short, N2B isoform may in principle serve as a mechanism to compensate for the large contour-length difference between the two isoforms. Simulation results of the effect of variation in the number of extra Ig domains in the N2BA isoform on apparent elasticity (before the onset of domain unfolding) of a titin doublet containing an N2B and an N2BA isoform are shown in Fig. 6c, inset. An increase in the number of extra Ig domains (69 vs. 56) in the N2BA isoform results in an increase of apparent persistence length of the entire bi-molecular oligomer, resulting in a noticeable, albeit little, decrease in the force for the given sarcomere length. Thus, by varying the contour lengths of the component chains via sequence insertions, and by shifting the ratios of titin isoforms with different effective contour lengths, the passive force vs. sarcomere-length relationship of striated muscle may be especially finely tuned.

Acknowledgements

This work was supported by grants from the National Institute of Health National Heart, Lung, and Blood Institute (HL61497 and HL62881) to H.L.G., GM32543 to C.B., and from the Hungarian Science Foundation (OTKA T037935) and European Union (HPRN-CT-2000-00091) to M.S.Z.K. M.S.Z.K. is a Howard Hughes Medical Institute International Research Scholar, and H.L.G. is an Established Investigator of the American Heart Association.

References

[1] R. Horowits, E.S. Kempner, M.E. Bisher, R.J. Podolsky, Nature 323 (1986) 160–164.
[2] R. Horowits, R.J. Podolsky, J. Cell Biol. 105 (1987) 2217–2223.
[3] H.L. Granzier, T.C. Irving, Biophys. J. 68 (1995) 1027–1044.
[4] C.C. Gregorio, H. Granzier, H. Sorimachi, S. Labeit, Curr. Opin. Cell Biol. 11 (1999) 18–25.
[5] H. Granzier, S. Labeit, J. Physiol. 541 (2002) 335–342.
[6] L. Tskhovrebova, J. Trinick, Philos. Trans. R. Soc. Lond., B Biol. Sci. 357 (2002) 199–206.
[7] D.O. Fürst, M. Osborn, R. Nave, K. Weber, J. Cell Biol. 106 (1988) 1563–1572.
[8] S. Labeit, B. Kolmerer, Science 270 (1995) 293–296.
[9] H. Granzier, M. Helmes, K. Trombitás, Biophys. J. 70 (1996) 430–442.
[10] W.A. Linke, M. Ivemeyer, N. Olivieri, B. Kolmerer, J.C. Ruegg, S. Labeit, J. Mol. Biol. 261 (1996) 62–71.
[11] K. Trombitás, J.P. Jin, H. Granzier, Circ. Res. 77 (1995) 856–861.
[12] O. Cazorla, A. Freiburg, M. Helmes, T. Centner, M. McNabb, Y. Wu, K. Trombitas, S. Labeit, H. Granzier, Circ. Res. 86 (2000) 59–67.
[13] M.S.Z. Kellermayer, H.L. Granzier, FEBS Lett. 380 (1996) 281–286.
[14] A. Soteriou, M. Gamage, J. Trinick, J. Cell. Sci. 104 (1993) 119–123.
[15] C.J. Bustamante, J.F. Marko, E.D. Siggia, S.B. Smith, Science 265 (1994) 1599–1600.
[16] J.F. Marko, E.D. Siggia, Macromolecules 28 (1995) 8759–8770.
[17] M.S.Z. Kellermayer, S.B. Smith, H.L. Granzier, C. Bustamante, Science 276 (1997) 1112–1116.
[18] M.S. Kellermayer, S.B. Smith, C. Bustamante, H.L. Granzier, Biophys. J. 80 (2001) 852–863.
[19] C. Rivetti, M. Guthold, C. Bustamante, J. Mol. Biol. 264 (1996) 919–932.
[20] M.S.Z. Kellermayer, S. Smith, C. Bustamante, H.L. Granzier, Adv. Exp. Med. Biol. 481 (2000) 111–126.
[21] R. Nave, D.O. Fürst, K. Weber, J. Cell Biol. 109 (1989) 2177–2187.
[22] H. Higuchi, Y. Nakauchi, K. Maruyama, S. Fujime, Biophys. J. 65 (1993) 1906–1915.
[23] G.I. Bell, Science 200 (1978) 618–627.
[24] M. Rief, J.M. Fernandez, H.E. Gaub, Phys. Rev. Lett. 81 (1998) 4764–4767.
[25] M. Rief, M. Gautel, A. Schemmel, H.E. Gaub, Biophys. J. 75 (1998) 3008–3014.
[26] M. Rief, M. Gautel, F. Oesterhelt, J.M. Fernandez, H.E. Gaub, Science 276 (1997) 1109–1112.
[27] H. Granzier, M. Kellermayer, M. Helmes, K. Trombitás, Biophys. J. 73 (1997) 2043–2053.
[28] K. Trombitás, M. Greaser, S. Labeit, J.P. Jin, M. Kellermayer, M. Helmes, H. Granzier, J. Cell Biol. 140 (1998) 853–859.
[29] M.S.Z. Kellermayer, S.B. Smith, C. Bustamante, H.L. Granzier, J. Struct. Biol. 122 (1998) 197–205.
[30] L. Tskhovrebova, J. Trinick, J. Mol. Biol. 265 (1997) 100–106.
[31] L. Tskhovrebova, J. Trinick, J. Mol. Biol. 310 (2001) 755–771.
[32] K. Wang, R. Ramirez-Mitchell, D. Palter, Proc. Natl. Acad. Sci. U. S. A. 81 (1984) 3685–3689.
[33] J. Trinick, P. Knight, A. Whiting, J. Mol. Biol. 180 (1984) 331–356.
[34] T. Funatsu, E. Kono, H. Higuchi, S. Kimura, S. Ishiwata, T. Yoshioka, K. Maruyama, S. Tsukita, J. Cell Biol. 120 (1993) 711–724.
[35] S. Improta, A.S. Politou, A. Pastore, Structure 4 (1996) 323–337.
[36] L. Tskhovrebova, J. Trinick, J.A. Sleep, R.M. Simmons, Nature 387 (1997) 308–312.
[37] K. Watanabe, C. Muhle-Goll, M.S. Kellermayer, S. Labeit, H. Granzier, J. Struct. Biol. 137 (2002) 248–258.
[38] M. Carrion-Vazquez, P.E. Marszalek, A.F. Oberhauser, J.M. Fernandez, Proc. Natl. Acad. Sci. U. S. A. 96 (1999) 11288–11292.
[39] H. Li, A.F. Oberhauser, S.D. Redick, M. Carrion-Vazquez, H.P. Erickson, J.M. Fernandez, Proc. Natl. Acad. Sci. U. S. A. 98 (2001) 10682–10686.
[40] K. Watanabe, P. Nair, D. Labeit, M.S. Kellermayer, M. Greaser, S. Labeit, H. Granzier, J. Biol. Chem. 277 (2002) 11549–11558.
[41] K. Trombitás, M. Greaser, G. French, H. Granzier, J. Struct. Biol. 122 (1998) 188–196.
[42] K. Trombitás, J.C. Wu, D. Labeit, S. Labeit, H.L. Granzier, Am. J. Physiol. 281 (2001) H1793–H1799.
[43] A.D. Liversage, D. Holmes, P.J. Knight, L. Tskhovrebova, J. Trinick, J. Mol. Biol. 305 (2001) 401–409.
[44] H.L. Granzier, K. Wang, Electrophoresis 14 (1993) 56–64.
[45] A. Freiburg, K. Trombitas, W. Hell, O. Cazorla, F. Fougerousse, T. Centner, B. Kolmerer, C. Witt, J.S. Beckmann, C.C. Gregorio, H. Granzier, S. Labeit, Circ. Res. 86 (2000) 1114–1121.